Observation of optical absorption correlated with surface state of topological insulator

Jiwon Jeon,[1] Kwangnam Yu,[1] Jiho Kim,[1,*] Jisoo Moon,[2] Seongshik Oh,[2] and E. J. Choi[1,†]

[1]*Department of Physics, University of Seoul, Seoul 130-743, Korea*

[2]*Department of Physics and Astronomy, Rutgers, The State University of New Jersey, Piscataway, New Jersey 08854, USA*

(Received 17 June 2019; published 7 November 2019)

We performed broadband optical transmission measurements of Bi_2Se_3 and In-doped $(Bi_{1-x}In_x)_2Se_3$ thin films, where in the latter the spin-orbit coupling (SOC) strength can be tuned by introducing In. Drude and interband transitions exhibit In-dependent changes that are consistent with evolution from the metallic ($x = 0$) to insulating ($x = 1$) nature of the end compounds. Most notably, an optical absorption peak located at $\hbar\omega = 1$ eV in Bi_2Se_3 is completely quenched at $x = 0.06$, the critical concentration where the phase transition from TI into non-TI takes place. For this x, the surface state (SS) has vanished from the band structure as well. The correlation between the 1 eV optical peak and the SS in the x dependencies suggests that the peak is associated with the SS. We further show that when Bi_2Se_3 is electrically gated, the 1 eV peak becomes stronger (weaker) when electron is depleted from (accumulated into) the SS. These observations combined together demonstrate that under the $\hbar\omega = 1$ eV illumination electron is excited from a bulk band into the topological surface band of Bi_2Se_3. The optical population of the surface band is of significant importance not only for fundamental study but also for TI-based optoelectronic device application.

DOI: 10.1103/PhysRevB.100.195110

I. INTRODUCTION

Topological insulator (TI) is a novel state of matter characterized by insulating bulk and metallic surface [1–5]. The surface state, topologically protected and chirally textured, supports dissipationless spin-conserving current, applicable for quantum devices [6–8]. Optically, various kinds of electron transitions occur in a TI under photo illumination both in the surface and in the bulk as demonstrated by numerous previous experiments: For the archetypal TI material Bi_2Se_3, intraband (Drude) transition and Kerr rotation of the surface carrier were observed in THz measurement [9]. In the infrared range, Post *et al.* measured the interband transition from bulk valence-band (VB) to bulk conduction-band (CB), VB → CB, and determined upper bound of Drude weight of SS [10]. Also Falsetti *et al.* observed the infrared Berreman resonance of the surface electron in Bi_2Se_3 thin films [11]. On the other hand, for periodically modulated Bi_2Se_3, plasmonic excitation of the surface electron [12] and the plasmon-phonon interaction [13] were observed at THz frequencies.

One interesting optical absorption that TI can host yet has not been detected is an excitation of an electron from bulk band into SS. This particular transition between bulk and surface, VB → SS, will provide a rare opportunity to study how the surface and bulk are connected optically. Also, when the surface electron is populated by this optical transition, the surface electron is increased and therefore the topological current ($\propto$ surface electron) is enhanced, which can boost the performance of TI as an optoelectronic device such as photogalvanics and optical imaging display [14,15]. In fact, Sobota *et al.* showed that a similar transition can occur from bulk CB to second SS, CB → 2nd SS, at a visible frequency [16]. (Here the second SS refers to another SS that lies above the first or fundamental SS). However, the optical transition into the first SS or fundamental SS, VB → SS, was not reported yet. It is not clear at this point whether the lack of the SS-populating optical transition is due to that other transition such as VB → CB is overwhelmingly stronger, making the detection difficult [17], or more fundamentally, this particular transition is forbidden by the optical selection rule.

Here we performed broadband optical absorption measurement of Bi_2Se_3 and $(Bi_{1-x}In_x)_2Se_3$ thin films from far-IR to UV frequencies. In $(Bi_{1-x}In_x)_2Se_3$, the spin-orbit coupling (SOC) strength is modulated by means of the indium (In) substitution. As In content is increased the SOC of Bi_2Se_3 is decreased and consequently the topological property is softened. Eventually, at a certain substitution level, the topological SS is completely quenched from the band structure. Accordingly any SS-related optical transition will be removed from the wide-range optical excitation spectrum, which in fact offers us an invaluable means to find the SS-population transition in particular. Our measurement shows signatures that such optical absorption may exist.

II. EXPERIMENT

High quality epitaxial Bi_2Se_3 and $(Bi_{1-x}In_x)_2Se_3$ thin films were grown on Al_2O_3 and SiO_2/Si substrates using the MBE method [18]. Optical transmittance $T(\omega)$ was measured from far-infrared to UV by using a Fourier transform infrared spectroscopy (FTIR) spectrometer in combination with a spectroscopic ellipsometer. For gate-dependent optical measurement gate-voltage V_G was applied between Bi_2Se_3 and Si of the substrate. Optical conductivity $\sigma_1(\omega)$ was calculated from

*Current address: 12D IRS Beamline, Pohang Accelerator Laboratory, Pohang 37673, Republic of Korea.

†echoi@uos.ac.kr

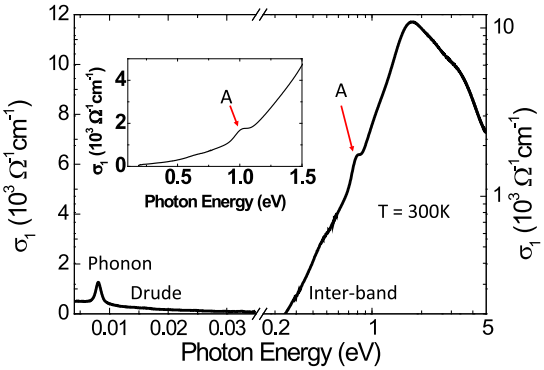

FIG. 1. Optical conductivity of Bi_2Se_3 thin film ($d = 50$ QL) $\sigma_1(\omega)$ shows the Drude, phonon, and interband transition. Note that log-log scale is used for the $0.2 \leqslant \hbar\omega \leqslant 5$ eV range. Inset shows peak A in the real scale.

transmission data through rigorous Kramers-Kronig transformation by using RefFit [19]. The experimental details are described in the Supplemental Material [20] and references therein.

III. RESULTS

Figure 1 shows the wide-range optical conductivity $\sigma_1(\omega)$ of the 50-QL-thick Bi_2Se_3 film. In the far-infrared region, $\sigma_1(\omega)$ consists of Drude absorption and optical phonon peak, both coming from the bulk, where the former one arises from the Se-vacancy driven carrier [21,22]. For $\hbar\omega > 0.25$ eV, the interband (IB) transition VB $\rightarrow$ CB leads to the rapid rise of $\sigma_1(\omega)$. Note that there is an absorption peak at $\hbar\omega = 1$ eV ($\equiv$ peak A hereafter) which we will pay particular attention to.

In Fig. 2 we show optical conductivity measured for a series of In-substituted $(Bi_{1-x}In_x)_2Se_3$ films. The In-concentration x was varied for the $0 \leqslant x \leqslant 0.9$ range. Previous studies showed that as Bi is replaced by the light element In, the spin-orbit interaction is reduced and the topological property of Bi_2Se_3 becomes weaker [23–26]. At a critical concentration x_c, phase transition from TI to non-TI (NTI) phase occurs where the bulk band gap is closed, and CB and VB begin to re-invert. The x_c lies between $x = 0.04$ and $x = 0.06$ depending on the film thickness, and for $x \geqslant x_c$ the topological SS has completely vanished [23,24]. The $\sigma_1(\omega)$ shows that peak A becomes weaker as x increases. For quantitative analysis of this behavior we isolate peak A by removing background conductivity from $\sigma_1(\omega)$ as $\sigma_1^A(\omega) = \sigma_1(\omega) - \sigma_1^{BG}(\omega)$ as illustrated in the inset of Fig. 2(d) (a polynomial function was used for the σ_1^{BG}), and calculated the strength of peak A as $S = \int \sigma_1^A(\omega)d\omega$. Figure 2(d) shows that S is quenched at $x = 0.06$. To double check this behavior we performed independent analysis of peak A: We calculate the second derivative $\frac{d^2\sigma_1}{dE^2}$ and measure the distance (w) and

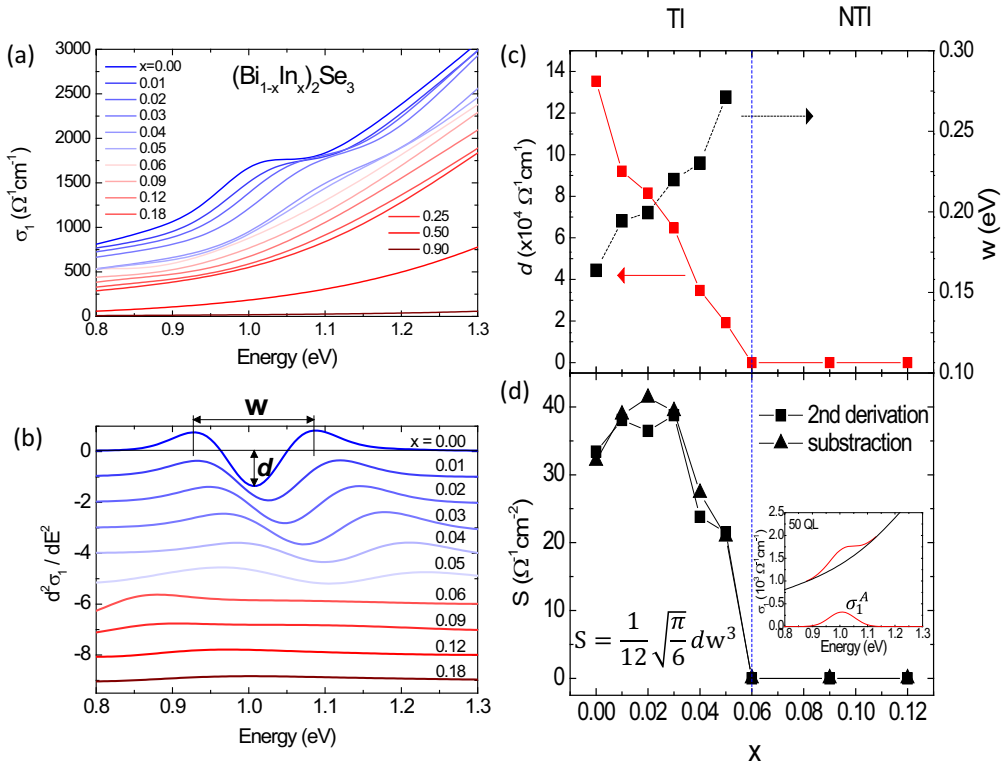

FIG. 2. Evolution of peak A in In-substituted $(Bi_{1-x}In_x)_2Se_3$ thin films. (a) Optical conductivity of $(Bi_{1-x}In_x)_2Se_3$ for the In-concentration range of $0 \leqslant x \leqslant 0.9$. (b) The second derivative of optical conductivity $\frac{d^2\sigma_1}{dE^2}$. The x-dependent behavior of peak A can be traced more clearly in this plot. Here w and d denote the distance between the two maxima and depth of the dip, respectively. (c) The width w and depth d are shown as a function of x. (d) The peak strength S calculated from $S = \frac{1}{12}\sqrt{\frac{\pi}{6}}dw^3$ (see Supplemental Material Fig. S1 [20]). We also calculate S by $S = \int \sigma_1^A(\omega)d\omega$, where $\sigma_1^A(\omega) = \sigma_1(\omega) - \sigma_1^{BG}(\omega)$ (σ_1^{BG} = polynomial background) as shown in the inset. In (c) and (d), the critical concentration $x_c = 0.06$ of the TI to non-TI (NTI) phase transition is highlighted by the vertical line.

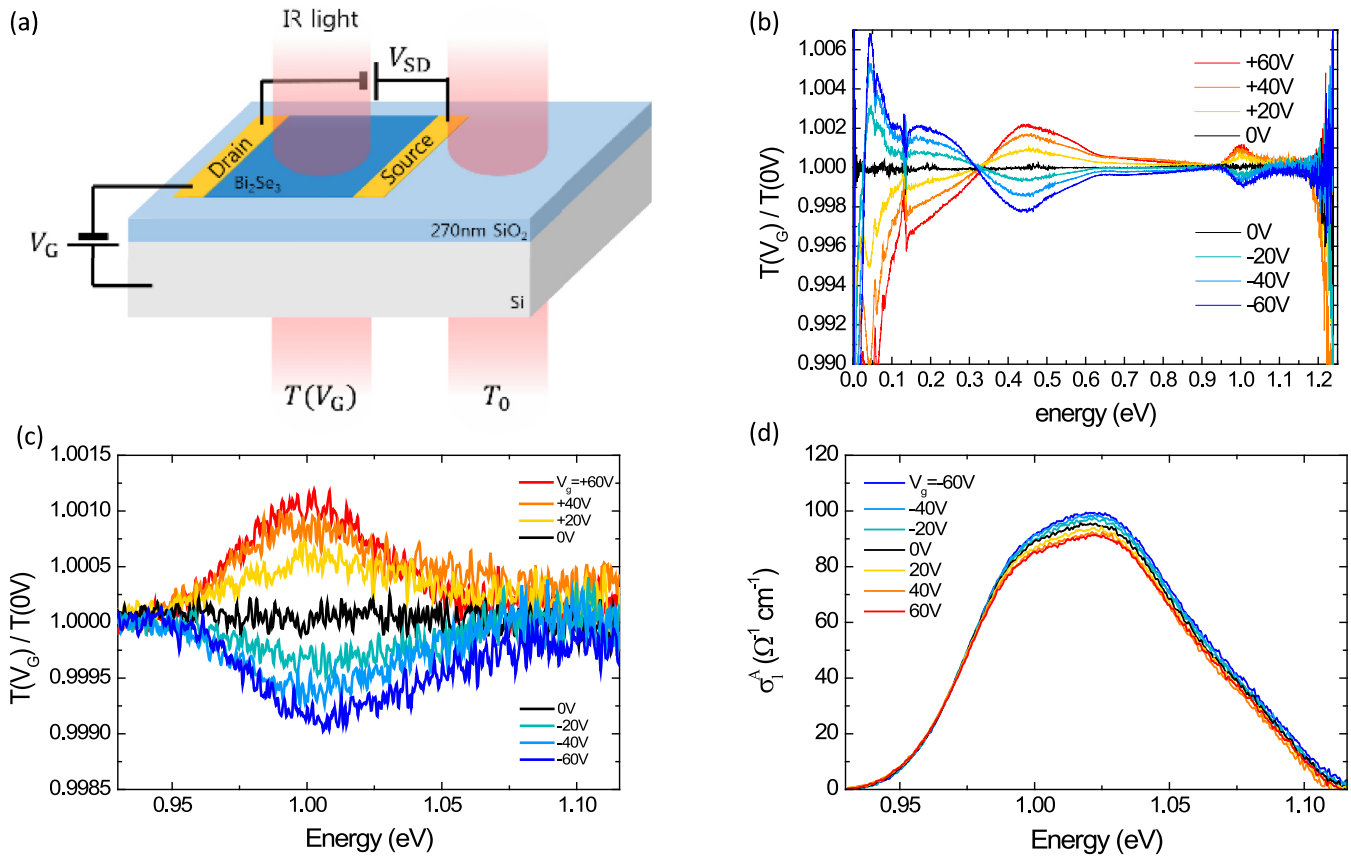

FIG. 3. Gate-driven change of Bi_2Se_3. (a) Schematic diagram of gate-controlled transmission measurement of Bi_2Se_3 thin film. $T(V_G)$ is taken with the bias voltage V_G applied between the film and Si. (b) $T(V_G)/T(0)$ changes in the far-IR, mid-IR, and at 1 eV. (c) For peak A $T(V_G)$ increases/decreases for the negative/positive V_G, respectively. (d) Optical conductivity of peak A, $\sigma_1^A(\omega)$, was calculated from $T(V_G)$ in (c) as described in the text.

depth (d) of the extrema pattern, which allows determination of strength S ($=\frac{1}{12}\sqrt{\frac{\pi}{6}}dw^3$) as well as width ($=\frac{1}{\sqrt{3}}w$) and height ($=\frac{1}{12}\,dw^2$) of peak A. (See Supplemental Material Fig. S1 for details [20].) The S is quenched at $x = 0.06$ again, which confirms the $S = \int \sigma_1^A(\omega)d\omega$ analysis. Importantly $x = 0.06$ is the critical x_c for the TI $\rightarrow$ NTI transition for the thickness $d = 50$ QL of our films: That is, the SS has vanished at this x. This correlation of peak A with the TI $\rightarrow$ NTI transition strongly suggests that peak A is related to the topological SS of Bi_2Se_3. We emphasize that this behavior is strikingly different from those of the other optical absorption features: In Supplemental Material Fig. S2 [20] we show that the Drude absorption has vanished at $x \sim 0.5$, the phonon peak splits at $x = 0.12$, and the IB survives up to $x = 0.9$. (For $x = 1$, In_2Se_3 is a large gap band insulator with $E_g > 1.5$ eV.) Note that none of these features are correlated with x_c. In contrast, peak A manifests a clear correlation with x_c and is the only absorption of its kind.

Given the correlation of peak A with SS, one can propose possible pictures on how peak A is created. Specifically, peak A can arise when (1) an SS electron is excited into an empty state lying 1 eV above, or alternatively (2) an electron lying at 1 eV below is excited into the SS. In both scenarios peak A becomes extinct when SS is suppressed at x_c. To find out which scenario is correct, we performed an electrical gating experiment on the Bi_2Se_3 film ($d = 8$ QL). For this a Bi_2Se_3 film was grown on SiO_2/Si substrate and optical transmission was measured while gate voltage V_G is applied between the film and Si. In this back-gate configuration, the Fermi energy E_F shifts down (up) for the negative (positive) V_G due to electron depletion (accumulation) in the film. Figure 3(b) shows that $T(V_G)/T(0)$ changes in the far-IR, mid-IR, and at 1 eV. Figure 3(c) shows that peak A becomes stronger (weaker) for negative (positive) V_G. Such change supports scenario (2) over (1) for the following reason: For $V_G < 0$ the electron occupation of SS is reduced and more empty SS become available, which strengthens the transition of (2), which agrees with the increase of peak-A strength. This relation is visualized in Fig. 4. In scenario (1), on the other hand, the surface electron is decreased and the peak becomes weaker, opposite to the observed behavior of peak A. Therefore, the V_G-dependent result demonstrates that peak A arises most likely by excitation of an electron from a state lying 1 eV below into the SS. In this transition electron occupation of SS is increased, or equally, the SS is optically populated by illuminating Bi_2Se_3 with $\hbar\omega = 1$ eV. Here we remark that the V_G-dependent change in Fig. 3(c) is very small, less than even 0.1%. Nevertheless the peak-A change is successfully measured, demonstrating the superior sensitivity and stability of our experiment. For later analysis we calculate the

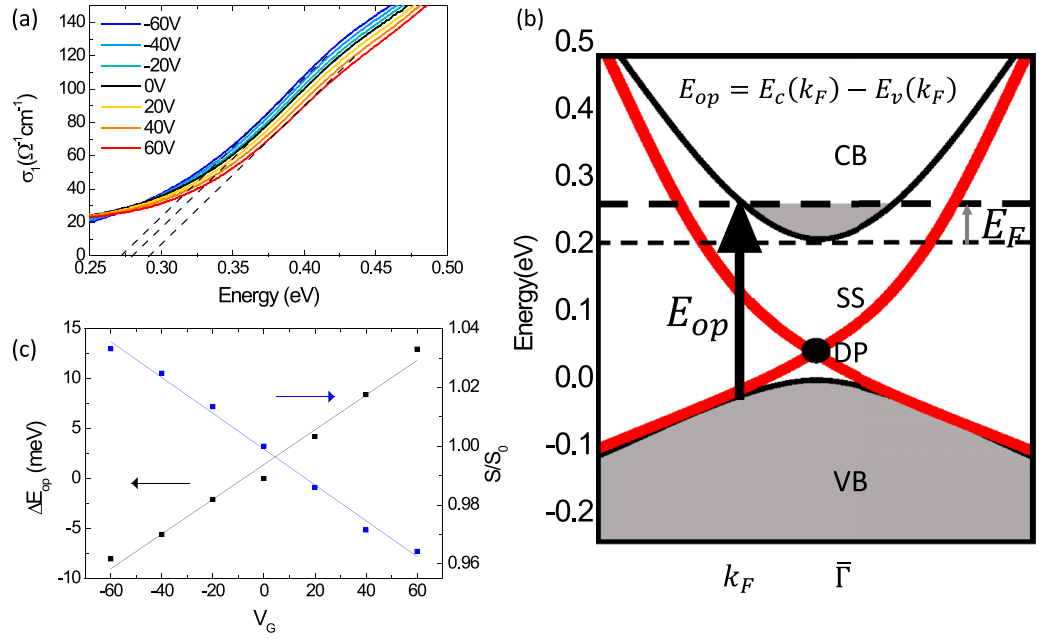

FIG. 4. Estimation of the growth of peak A at high gating voltage. (a) Gate-driven shift of the interband transition. The onset energy $E_{\rm op}$ is determined by the linear extrapolation of data (dashed line). (b) Schematic diagram of the VB $\rightarrow$ CB interband transition. The $E_{\rm op}$ corresponds to onset of the VB $\rightarrow$ CB. Here the Fermi energy $E_{\rm F}$ is measured from the CB bottom. DP stands for Dirac point. (c) The shift $\Delta E_{\rm op} = E_{\rm op}(V_{\rm G}) - E_{\rm op}(0)$ and the change of S are plotted against $V_{\rm G}$. Here S was calculated by integrating $\sigma_1(\omega)$ in Fig. 3(c) as $S = \int \sigma_1^A(\omega) d\omega$.

$V_{\rm G}$-dependent $\sigma_1(\omega)$ from the $T(V_{\rm G})/T(0)$ data [27–29] and show it in Fig. 3(d).

With the nature of peak A identified, the next question to be addressed is the origin of the initial state. Before we discuss this issue, we give further thoughts on the gate-dependent growth of peak A. Figure 3 implies that the SS population will become stronger if $E_{\rm F}$ could be brought down further. The latter would be possible when $V_{\rm G}$ is applied to a high value beyond the limit of our measurement, where such high gating was in fact demonstrated experimentally [30]. Here we will consider how large peak A will grow in the strong-gating regime. In Fig. 4(a) we show the bulk interband transition in the mid-IR range. The onset energy ($\equiv E_{\rm op}$) of this transition corresponds to the thick arrow in Fig. 4(b). The $E_{\rm op}$ increases when the Fermi level shifts up. Figure 4(c) shows that the increase rate is $dE_{\rm op}/dV_{\rm G} = 1.74 \times 10^{-4}$ (eV/V) $\equiv a$. In the meantime the $S = \int \sigma_1^A(\omega) d\omega$ calculated from Fig. 3(d) decreases at the rate $ds/dV_{\rm G} = -6.06 \times 10^{-4}$ (1/V) $\equiv b$, where $s = S/S$ (0 V) is the normalized S by ungated $S(0)$. Given a and b we can eliminate $V_{\rm G}$ and obtain the S change against $E_{\rm F}$ as $ds/dE_{\rm F} = (ds/dV_{\rm G})(dV_{\rm G}/dE_{\rm F}) = b/(a/2) = 6.96$ (1/eV). Here $dV_{\rm G}/dE_{\rm F} = (a/2)^{-1}$ was derived by utilizing the Bernstein-Moss relation [31–33], namely $dE_{\rm F}/dV_G = \frac{1}{2} dE_{\rm op}/dV_{\rm G} = \frac{a}{2}$, where the factor $\frac{1}{2}$ comes from $\frac{1}{m^*_{\rm CV}} = \frac{1}{m^*_{\rm CB}} + \frac{1}{m^*_{\rm VB}}$ and $m^*_{\rm CB} = m^*_{\rm VB}$ [34]. This result $ds/dE_{\rm F} = 6.96$ (1/eV) enables us to estimate S at high gating: For the pristine, electron-doped Bi_2Se_3 films like ours, the Fermi level lies typically at $E_{\rm F} \sim 0.1$ eV from the CB bottom (CBB). If the gating shifts $E_{\rm F}$ down to the CBB, i.e., $\Delta E_{\rm F} = 0.1$, then s will increase approximately by $\Delta s \approx [\frac{ds}{dE_{\rm F}}]\Delta E_{\rm F} = 0.69$. That is, peak A grows by ~70% compared with the ungated strength. If $E_{\rm F}$ is shifted further to the Dirac point, the latter lying ~0.2 eV from the CBB, we have $s = s(0) + \Delta s \approx 1 + [\frac{ds}{dE_{\rm F}}](0.1 + 0.2) = 3.09$. That is, peak A grows as large as three times. (Here we assumed $\frac{ds}{dE_{\rm F}}$ is constant for simplicity, neglecting its $E_{\rm F}$ dependence.) This estimation shows that substantial increase of the peak will occur at high gating. From this exercise we also learn that if S is precisely characterized as a function of $E_{\rm F}$, it could be used to determine the location of the Fermi level in Bi_2Se_3 films, whereas usually more difficult ARPES should be performed.

IV. DISCUSSION

We now search for a possible candidate for the initial state of peak A. For this we refer to the band structure of Bi_2Se_3 reported in experimental [3,7,35–39] and theoretical [40–43] literatures, and schematically redrew it in Fig. 5. In Fig. 5 note that there is an energy branch lying ~1 eV below the SS. Interestingly, this branch $E(k)$ runs in near parallel with the SS. If we consider the optical transition from this $E(k)$ branch ($=i$) to SS ($=f$), their parallel dispersion $\nabla_k E^i(k) \cong \nabla_k E^f(k)$ leads to strong absorption due to that transition strength $S \sim \int \frac{M_{fi}}{|\nabla_k E^f(k) - \nabla_k E^i|} d^2k$ becomes divergent. This yields a pronounced absorption at $\hbar\omega = E_f - E_i = 1$ eV, which agrees with the profile of peak A. (Here the transition matrix element M_{fi} is assumed to be constant for simplicity.) Therefore this 1 eV $E(k)$ is a plausible candidate for the i state. We think that this assignment can be confirmed when theoretical calculation of $\sigma_1(\omega)$, not available currently, is performed. We remark that optical transition of Bi_2Se_3 between bulk and surface in particular was poorly studied so

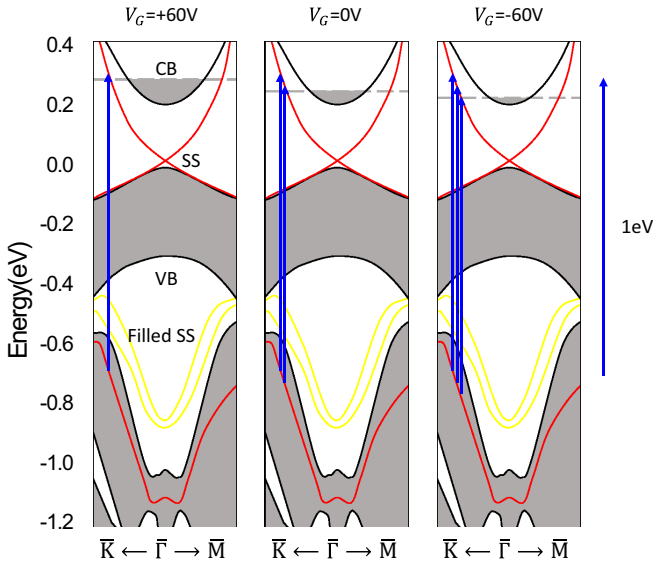

FIG. 5. Schematic band structure and possible origin of peak A. For $V_G = 0$, an electron is excited from the bulk band branch into the empty surface state as highlighted by the blue arrows. For the positive gating, the Fermi level E_F shifts up and the 1 eV transition becomes weaker. For the negative gating E_F shifts down and the 1 eV transition becomes stronger. The amount of E_F shift is exaggerated for clarity. The band diagram shown here was redrawn schematically based on experiment [3,7,35–39] and theory [40–43]. CB = bulk conduction band, VB = bulk valence band, SS = surface state.

far with a rare exception [17]. To consider another candidate, a native defect such as Se vacancy can produce defect levels below E_F. However, their energy locations are not well known, and generally such localized, dispersionless levels do not fulfill the $\nabla_k E^i(k) \cong \nabla_k E^f(k)$ condition. We emphasize that, while supporting works should follow to definitely identify the 1 eV bulk $E(k)$ as origin of i state, the occurrence of the optical population of SS in Bi_2Se_3 is evident judging from the properties of peak A we have unveiled regardless of the i-state origin.

To make a further remark on the $T(V_G)/T(0)$ data, Fig. 3(b) shows that gate-dependent change occurs in the far-IR and mid-IR ranges also. Similar change was reported for bulk-insulating $(Bi_{1-x}In_x)_2Se_3$ films [44]. While for $(Bi_{1-x}Sb_x)_2Te_3$ the mid-IR modulation peaks at ∼0.3 eV, the modulation for Bi_2Se_3 occurs at higher energy, peaked at 0.45 eV. This difference is attributed to that the interband transition taking place at $E_{op} = E_g + 2E_F$ is higher for Bi_2Se_3 where E_F is significant (∼0.1 eV) compared with the insulating $(Bi_{1-x}Sb_x)_2Te_3$ where E_F is considered to be much lower. Also, while the modulations in mid-IR and far-IR inevitably contain contribution from both bulk and surface states, the modulation strength of the 1 eV feature is weaker, which may further support the surface-related origin. Further quantitative analysis and comparison will be published separately.

In conclusion, we performed broadband optical absorption measurement on pristine Bi_2Se_3 and In-substituted $(Bi_{1-x}In_x)_2Se_3$ thin films, as well as electrically gated Bi_2Se_3. The absorption peak A that occurs at $\hbar\omega = 1$ eV showed clear correlation with the In-driven TI-NTI phase transition: It is activated at $x < x_c$ (TI phase) but has completely vanished for $x > x_c$ (NTI) along with the quenching of the topological surface state. Furthermore, peak A become stronger/weaker by the electron depletion/injection into the Bi_2Se_3 in the electrical gating measurement. The two experimental results provide convincing evidence that peak A arises from the population of SS, i.e., the optical excitation of an electron from 1 eV below into the SS. This SS-optical population increases the density of the surface electron, and thus can enhance the topological electrical conduction, which promotes TI device application. Similar optically driven SS population may be realized in other TI materials as well, which should be investigated in the future.

Note added. For our $(Bi_{1-x}In_x)_2Se_3$ films, the bulk transition E_{op} shows a different x-dependent behavior from Ref. [25]. It may come from that carrier doping due to Se vacancy is sample dependent for these TI films. See Supplemental Material Fig. S3 [20].

ACKNOWLEDGMENTS

This work was supported by the 2016 sabbatical year research grant of the University of Seoul and the National Research Foundation of Korea (NRF-2017R1A2B4007782). J.M. and S.O. are supported by the Gordon and Betty Moore Foundation's EPiQS Initiative (Grant No. GBMF4418) and National Science Foundation (NSF) Grant No. EFMA-1542798.

[1] L. Fu, C. L. Kane, and E. J. Mele, Phys. Rev. Lett. **98**, 106803 (2007).
[2] Y. Xia, D. Qian, D. Hsieh, L. Wray, A. Pal, H. Lin, A. Bansil, D. Grauer, Y. S. Hor, R. J. Cava *et al.*, Nat. Phys. **5**, 398 (2009).
[3] M. Z. Hasan and C. L. Kane, Rev. Mod. Phys. **82**, 3045 (2010).
[4] J. E. Moore, Nature (London) **464**, 194 (2010).
[5] X.-L. Qi and S.-C. Zhang, Rev. Mod. Phys. **83**, 1057 (2011).
[6] P. Roushan, J. Seo, C. V. Parker, Y. S. Hor, D. Hsieh, D. Qian, A. Richardella, M. Z. Hasan, R. J. Cava, and A. Yazdani, Nature (London) **460**, 1106 (2009).
[7] D. Hsieh, Y. Xia, D. Qian, L. Wray, J. Dil, F. Meier, J. Osterwalder, L. Patthey, J. Checkelsky, N. Ong *et al.*, Nature (London) **460**, 1101 (2009).
[8] C. Li, O. Vant Erve, J. Robinson, Y. Liu, L. Li, and B. Jonker, Nat. Nanotechnol. **9**, 218 (2014).
[9] R. Valdes Aguilar, A. V. Stier, W. Liu, L. S. Bilbro, D. K. George, N. Bansal, L. Wu, J. Cerne, A. G. Markelz, S. Oh, and N. P. Armitage, Phys. Rev. Lett. **108**, 087403 (2012).
[10] K. W. Post, B. C. Chapler, M. K. Liu, J. S. Wu, H. T. Stinson, M. D. Goldflam, A. R. Richardella, J. S. Lee, A. A. Reijnders, K. S. Burch, M. M. Fogler, N. Samarth, D. N. Basov *et al.*, Phys. Rev. Lett. **115**, 116804 (2015).
[11] E. Falsetti, A. Nucara, P. P. Shibayev, M. Salehi, J. Moon, S. Oh, J.-B. Brubach, P. Roy, M. Ortolani, and P. Calvani, Phys. Rev. Lett. **121**, 176803 (2018).

[12] P. Di Pietro, M. Ortolani, O. Limaj, A. Di Gaspare, V. Giliberti, F. Giorgianni, M. Brahlek, N. Bansal, N. Koirala, S. Oh *et al.*, Nat. Nanotechnol. **8**, 556 (2013).
[13] C. In, S. Sim, B. Kim, H. Bae, H. Jung, W. Jang, M. Son, J. Moon, M. Salehi, S. Y. Seo *et al.*, Nano Lett. **18**, 734 (2018).
[14] J. McIver, D. Hsieh, H. Steinberg, P. Jarillo-Herrero, and N. Gedik, Nat. Nanotechnol. **7**, 96 (2012).
[15] Z. Yue, G. Xue, J. Liu, Y. Wang, and M. Gu, Nat. Commun. **8**, 15354 (2017).
[16] J. A. Sobota, S.-L. Yang, A. F. Kemper, J. J. Lee, F. T. Schmitt, W. Li, R. G. Moore, J. G. Analytis, I. R. Fisher, P. S. Kirchmann, T. P. Devereaux, and Z. X. Shen, Phys. Rev. Lett. **111**, 136802 (2013).
[17] L. Li, W. Xu, and F. Peeters, J. Appl. Phys. **117**, 175305 (2015).
[18] N. Bansal, Y. S. Kim, E. Edrey, M. Brahlek, Y. Horibe, K. Iida, M. Tanimura, G.-H. Li, T. Feng, H.-D. Lee *et al.*, Thin Solid Films **520**, 224 (2011).
[19] A. Kuzmenko, Rev. Sci. Instrum. **76**, 083108 (2005).
[20] See Supplemental Material at http://link.aps.org/supplemental/10.1103/PhysRevB.100.195110 for additional data of the Bi_2Se_3 which includes Ref. [45].
[21] K. W. Post, B. C. Chapler, L. He, X. Kou, K. L. Wang, and D. N. Basov, Phys. Rev. B **88**, 075121 (2013).
[22] P. Di Pietro, F. M. Vitucci, D. Nicoletti, L. Baldassarre, P. Calvani, R. Cava, Y. S. Hor, U. Schade, and S. Lupi, Phys. Rev. B **86**, 045439 (2012).
[23] M. Brahlek, N. Bansal, N. Koirala, S.-Y. Xu, M. Neupane, C. Liu, M. Z. Hasan, and S. Oh, Phys. Rev. Lett. **109**, 186403 (2012).
[24] M. Salehi, H. Shapourian, N. Koirala, M. J. Brahlek, J. Moon, and S. Oh, Nano Lett. **16**, 5528 (2016).
[25] L. Wu, M. Brahlek, R. V. Aguilar, A. Stier, C. Morris, Y. Lubashevsky, L. Bilbro, N. Bansal, S. Oh, and N. Armitage, Nat. Phys. **9**, 410 (2013).
[26] S. Sim, N. Koirala, M. Brahlek, J. H. Sung, J. Park, S. Cha, M.-H. Jo, S. Oh, and H. Choi, Phys. Rev. B **91**, 235438 (2015).
[27] K. Yu, J. Kim, J. Y. Kim, W. Lee, J. Y. Hwang, E. H. Hwang, and E. J. Choi, Phys. Rev. B **94**, 235404 (2016).
[28] K. Yu, J. Jeon, J. Kim, C. W. Oh, Y. Yoon, B. J. Kim, J. H. Cho, and E. Choi, Appl. Phys. Lett. **114**, 083503 (2019).
[29] K. Yu, N. Van Luan, T. Kim, J. Jeon, J. Kim, P. Moon, Y. H. Lee, and E. Choi, Phys. Rev. B **99**, 241405 (2019).
[30] N. Bansal, N. Koirala, M. Brahlek, M.-G. Han, Y. Zhu, Y. Cao, J. Waugh, D. S. Dessau, and S. Oh, Appl. Phys. Lett. **104**, 241606 (2014).
[31] E. Burstein, Phys. Rev. **93**, 632 (1954).
[32] T. Moss, Proc. Phys. Soc. Sect. B **67**, 775 (1954).
[33] I. Hamberg, C. G. Granqvist, K.-F. Berggren, B. E. Sernelius, and L. Engström, Phys. Rev. B **30**, 3240 (1984).
[34] J. G. Analytis, J.-H. Chu, Y. Chen, F. Corredor, R. D. McDonald, Z. X. Shen, and I. R. Fisher, Phys. Rev. B **81**, 205407 (2010).
[35] I. A. Nechaev, R. C. Hatch, M. Bianchi, D. Guan, C. Friedrich, I. Aguilera, J. L. Mi, B. B. Iversen, S. Blügel, P. Hofmann, and E. V. Chulkov, Phys. Rev. B **87**, 121111(R) (2013).
[36] Z.-H. Pan, E. Vescovo, A. V. Fedorov, D. Gardner, Y. S. Lee, S. Chu, G. D. Gu, and T. Valla, Phys. Rev. Lett. **106**, 257004 (2011).
[37] L. A. Wray, S.-Y. Xu, Y. Xia, Y. San Hor, D. Qian, A. V. Fedorov, H. Lin, A. Bansil, R. J. Cava, and M. Z. Hasan, Nat. Phys. **6**, 855 (2010).
[38] A. Dubroka, O. Caha, M. Hronček, P. Friš, M. Orlita, V. Holý, H. Steiner, G. Bauer, G. Springholz, and J. Humlíček, Phys. Rev. B **96**, 235202 (2017).
[39] B. A. Piot, W. Desrat, D. K. Maude, M. Orlita, M. Potemski, G. Martinez, and Y. S. Hor, Phys. Rev. B **93**, 155206 (2016).
[40] I. Aguilera, C. Friedrich, G. Bihlmayer, and S. Blügel, Phys. Rev. B **88**, 045206 (2013).
[41] M. Guo, Z. Wang, Y. Xu, H. Huang, Y. Zang, C. Liu, W. Duan, Z. Gan, S.-C. Zhang, K. He *et al.*, New J. Phys. **18**, 015008 (2016).
[42] T. Förster, P. Krüger, and M. Rohlfing, Phys. Rev. B **91**, 035313 (2015).
[43] M. Hermanowicz and M. W. Radny, Phys. Status Solidi RRL **13**, 1800460 (2019).
[44] W. S. Whitney, V. W. Brar, Y. Ou, Y. Shao, A. R. Davoyan, D. N. Basov, K. He, Q.-K. Xue, and H. A. Atwater, Nano Lett. **17**, 255 (2016).
[45] A. LaForge, A. Frenzel, B. Pursley, T. Lin, X. Liu, J. Shi, and D. Basov, Phys. Rev. B **81**, 125120 (2010).